Title: Satellite-based evidence for shrub and graminoid tundra expansion in northern Quebec from 1986-2010.

Running Title: Shrub Expansion in Northern Quebec

Authors: K.M. McManus[1], D.C. Morton[2], J.G. Masek[2], D. Wang[3], J.O. Sexton[3], J. Nagol[3], P. Ropars[4], S. Boudreau[4]

Affiliations:
[1] Environmental Earth System Science, Stanford University
2 Biospheric Sciences Laboratory, NASA Goddard Space Flight Center
3 Department of Geographical Sciences, University of Maryland, College Park
4 Département de biologie, Northern Research Chair on Disturbance Ecology, Centre d'études nordiques, Université Laval

Corresponding Author: Kelly M. McManus, Stanford University, Department of Global Ecology. 260 Panama Ave, Stanford, CA 94305. email: mcmanusk@stanford.edu

Keywords: Arctic ecosystems, climate-induced vegetation response, Landsat, remote sensing, time-series analysis

Abstract

Global vegetation models predict rapid poleward migration of tundra and boreal forest vegetation in response to climate warming. Local plot and air-photo studies have documented recent changes in high-latitude vegetation composition and structure, consistent with warming trends. To bridge these two scales of inference, we analyzed a 24-year (1986-2010) Landsat time series in a latitudinal transect across the boreal forest-tundra biome boundary in northern Quebec province, Canada. This region has experienced rapid warming during both winter and summer months during the last forty years. Using a per-pixel (30 m) trend analysis, 30% of the observable (cloud-free) land area experienced a significant ($p < 0.05$) positive trend in the Normalized Difference Vegetation Index (NDVI). However, greening trends were not evenly split among cover types. Low shrub and graminoid tundra contributed preferentially to the greening trend, while forested areas were less likely to show significant trends in NDVI. These trends reflect increasing leaf area, rather than an increase in growing season length, because Landsat data were restricted to peak-summer conditions. The average NDVI trend (0.007/yr) corresponds to a leaf-area index (LAI) increase of ~0.6 based on the regional relationship between LAI and NDVI from the Moderate Resolution Spectroradiometer (MODIS). Across the entire transect, the area-averaged LAI increase was ~0.2 during 1986-2010. A higher area-averaged LAI change (~0.3) within the shrub-tundra portion of the transect represents a 20-60% relative increase in LAI during the last two decades. Our Landsat-based analysis subdivides the overall high-latitude greening trend into changes in peak-summer greenness by cover type. Different responses within and among shrub, graminoid, and tree-dominated cover types in this study indicate important fine-scale heterogeneity in vegetation growth. Although our findings are consistent with community shifts in low-biomass vegetation types over multi-decadal time

scales, the response in tundra and forest ecosystems to recent warming was not uniform.

1.0 Introduction

Climate exerts a primary control on the extent of forest cover and other vegetation types within Arctic and sub-Arctic ecosystems. Recent warming has been most rapid at high latitudes, and stronger warming expected in the next century may shift the distribution of vegetation types at these latitudes (IPCC 2007). Dynamic global vegetation models (DGVMs) predict a temperature-induced growth response in high-latitude ecosystems, leading to a poleward or upslope expansion of boreal forest and an increase in the boreal forest carbon sink over the course of the 21st century (Emanuel *et al.* 1985; Pastor & Post 1988; Prentice & Fung 1990; White *et al.* 2000; Parmesan & Yohe 2003; Lucht *et al.* 2006; IPCC 2007). In many of these scenarios, the vegetation response to warming is both widespread and rapid during the 21st century, which suggests that early signs of warming-induced biome shifts might already be observable.

Coarse-resolution satellite data and field observations have provided intriguing evidence for climate-driven shifts in vegetation type and condition since the mid-20th century. Vegetation index data from the coarse-resolution Advanced Very High Resolution Radiometer (AVHRR) have suggested widespread increases in high-latitude vegetation greenness and net primary productivity (NPP) since the 1980's (Myneni *et al.* 1997; Goetz *et al.* 2005; Bunn & Goetz 2006; Pouloit *et al.* 2009; Wang *et al.* 2011). AVHRR-based studies of high-latitude greening typically use seasonally-integrated vegetation indices. Thus, it is not clear whether these satellite-based "greening" trends reflect increased peak-summer vegetation cover or lengthening growing seasons (including trends in spring snow cover). These studies also lack the spatial resolution to

delineate stand-level changes in vegetation composition or extent (Masek 2001) and suffer to varying degrees from issues associated with instrument calibration and sampling (e.g., Running *et al.* 2004; Gallo *et al.* 2005).

Field studies using plot measurements or repeat aerial photography suggest that recent climate warming has led to expansion of shrub cover within tundra biomes (Van Wijk *et al.* 2004; Tape *et al.* 2006; Jagerbrand *et al.* 2006;Tremblay 2010; Ropars & Boudreau 2012). However, the extent to which such local trends contribute to or characterize larger, systemic change in Arctic and sub-Arctic vegetation remains unknown. Within the boreal forest biome, evidence for climate-driven change is less conclusive. A meta-analysis of pan-boreal treeline studies indicated that northward or altitudinal expansion of forest is evident in over half of study sites with coincident warming trends (Harsch *et al.* 2009), yet variation in treeline form (e.g. diffuse, abrupt, island, and krummolz) suggests a diversity of responses to local conditions as well as climate (Harsch & Bader 2011). Recent studies demonstrate the possibility to link field observations and satellite-based trends in vegetation productivity (e.g., Beck *et al.* 2011); however, higher-resolution satellite observations are likely needed to directly scale individual tree or stand-scale growth responses to satellite resolution. Large area coverage with high resolution time series is also desirable since coarse or moderate resolution satellite data indicate a diversity of trends in tundra ecosystems and primarily negative (browning) trends over boreal forest in North America (Bunn & Goetz 2006; Pouliot *et al.* 2009; Zhao & Running 2010).

In this study, we use fine-scale Landsat observations to quantify vegetation changes within and among plant cover types over the past quarter-century. Our study considers a latitudinal transect

across the forest-tundra biome boundary in northern Quebec, a region that has experienced rapid warming in both winter (November-April) and summer (May-October) seasons during the satellite era, from the early 1970s onwards (Fig. 1). Unlike previous satellite-based studies of vegetation greening, we carefully selected time series of peak-summer Landsat data to evaluate changes in vegetation composition and structure rather than changes in phenology. The study had three specific aims: 1) identify changes in high-latitude tundra and forest cover types over a period of pronounced warming using time series of Landsat Normalized Difference Vegetation Index (NDVI); 2) analyze the magnitude and distribution of change by cover type; and 3) assess the underlying ecological mechanisms of a trend in greenness by plant cover type and terrain attributes.

2.0 Materials and Methods

2.1 Data

We assembled a Landsat time series transect across the forest-tundra biome boundary in northern Quebec to assess changes in summer vegetation cover during 1986-2010 (Fig. 1). The transect spanned 9 adjacent Landsat frames, covering an area of 260,000 km^2. The time series of Landsat data for each frame in the transect was selected to minimize the impact of phenology on trends in summer vegetation cover over the 24-year period (Fig. 2). We used the average growing season phenology during 2001-2006 from the MODIS phenology product (MCD12Q2, Zhang *et al.* 2003) to select the peak growing season greenness for each Landsat data frame. Within this narrow window of peak greenness (day of year 185-215, or July 4 – August 3 in non-leap years), images were selected to minimize cloud cover and variability in the date of image acquisition. A total of 52 Landsat Thematic Mapper (TM) and Enhanced Thematic Mapper Plus (ETM+) images were acquired from the United States Geological Survey (glovis.usgs.gov) and Canadian Centre for Remote Sensing (ccrs.nrcan.gc.ca) Landsat Data Archives, with an average of 6 Landsat scenes per frame (Fig. 2).

Landsat data were converted from radiance to surface reflectance using the Landsat Ecosystem Disturbance Adaptive Processing System (LEDAPS), an automated atmospheric correction approach to account for absorption and scattering by atmospheric trace gases (O_3, O_2, CO_2, NO_2, and CH_4), aerosols, and water vapor (Masek *et al.* 2006). The LEDAPS system also generates a cloud mask layer. For this study, we implemented additional masking procedures for water (Band 4 reflectance <0.12), thin cirrus clouds (Band 1 reflectance >0.08), and contrails (Band 6

brightness temperatures). Finally, the Normalized Difference Vegetation Index (NDVI) was calculated from the masked red and near-infrared surface reflectance data for each scene (Tucker 1979). Time series of NDVI for each Landsat frame were used to detect trends in forest and tundra vegetation during 1986-2010.

Temperature trends in Boreal North America area were analyzed using monthly mean temperatures from the University of East Anglia Climatic Research Unit Time Series 3.1 (CRU TS3.1, http://badc.nerc.ac.uk/data/cru). The CRU TS3.1 product is a gridded 0.5° x 0.5° product based on meteorological station data (see Mitchell & Jones 2005). Monthly mean temperatures were averaged for winter (November-April) and summer (May-October) seasons; previous studies have shown that warming winter temperatures may be important for recent treeline advances (e.g., Harsch et al., 2009). Simple linear regression was used to estimate trends in mean winter and summer temperatures for 1971-2008 and 1970-2009, respectively. The total change in winter and summer temperatures during 1970-2009 was estimated using linear trends on a per-pixel basis. Finally, seasonal temperature changes were averaged for each 0.5° latitude bin to estimate the gradients in winter and summer temperatures within the Landsat transect during this period.

2.2 Trend Detection

Trends in mid-summer NDVI were assessed on a per-pixel basis using least-squares regression. For a time series of *n* scenes, only pixels with *n* or *n-1* observations were evaluated for trends in NDVI over time. Selecting pixels with one missing data value allowed for the use of some

154 cloud-filtered data and post-2003 Landsat ETM+ data while minimizing the potential for
155 spurious trend detection. In regions with overlapping coverage from adjacent Landsat frames,
156 the denser time series was selected to assess trends in NDVI over time. For each 30-meter pixel,
157 the slope and statistical significance of the linear regression in NDVI values were evaluated
158 using a Student's t-test at 95% confidence level.
159
160 Large-scale disturbances from fire and wood harvest are common in North American boreal
161 forests. Although climate warming may influence disturbance rates in boreal forests, the focus of
162 this work was to detect vegetation changes in undisturbed regions. Therefore, we used two
163 approaches to exclude large-scale disturbances from the analysis of NDVI trends. First, the
164 earliest cloud-free Landsat MSS image for each scene (1972-1976) was used to digitize burn scar
165 perimeters for fires prior to the start of each Landsat TM/ETM+ time series (~1986). These
166 areas were eliminated from further analysis. Second, within the Landsat TM/ETM+ time series
167 (1986-2010), a thresholding approach was used to eliminate areas with strong increases or
168 decreases in NDVI (absolute changes greater than 0.08 NDVI) between successive images.
169
170 The sensitivity of the Landsat NDVI trend detection approach to real changes in vegetation cover
171 depends, in part, on the uncertainty in the original radiometric observations (measurement
172 errors). Recent improvements to Landsat calibration, including cross calibration of Landsat-4, -5,
173 and -7 data using an absolute radiometric scale (Markham & Helder in press), have reduced
174 uncertainties associated with comparing Landsat data from different sensors. The uncertainty of
175 the LEDAPS atmospherically corrected products is the greater of 0.5% absolute reflectance or
176 5% of the recorded reflectance value (1σ), similar to the NASA Moderate Resolution Imaging

177 Spectroradiometer (MODIS) sensors (Masek *et al.* 2006). The resulting uncertainty in any given
178 NDVI observation is thus ~0.02 (1σ). Based on Monte Carlo modeling of MODIS NDVI trend
179 detection using noisy time series (Wang *et al.* 2012), we expect that actual NDVI trends greater
180 than ±0.003 NDVI yr^{-1} can be reliably mapped given the Landsat measurement errors and the
181 typical number of observations for each frame in the transect.
182
183 Increases in NDVI over time are generally associated with increases in leaf area index (LAI)
184 (Turner *et al.* 1999). Because changes in LAI may be more easily compared to modeled or
185 measured vegetation changes, we developed relationships between NDVI and LAI using the
186 MODIS/Aqua LAI product (MYD15A2, Knyazikhin *et al.* 1999) and NDVI product
187 (MYD13A1, Huete *et al.* 2002). First, trends in 2002-2010 MODIS LAI and NDVI were
188 assessed independently across the northern United States and Canada, using the same linear
189 regression and t-test approach as the analysis of trends in Landsat NDVI. Data quality layers
190 were used to restrict the analysis to LAI estimates from the radiative transfer algorithm and
191 highest quality NDVI observations. Pixels with statistically significant linear trends in both
192 MODIS LAI and MODIS NDVI were selected to derive estimates of the change in LAI per unit
193 NDVI. The larger (continental) geographic area allowed over 200,000 MODIS NDVI-LAI pairs
194 to be collected for comparison.
195
196 ***2.3 Spatial Analysis of NDVI Trends***
197 Trends in Landsat NDVI during 1986-2010 were assessed by cover type using forest and tundra
198 land cover classifications derived from circa 2000 Landsat imagery. North of the tree line,
199 designated as the Rivière aux Feuilles, tundra cover types were classified based on the CCRS

Northern Land Cover of Canada dataset (http://www.ccrs.nrcan.gc.ca/optical/landcover2000_e.php). The Canadian Forest Service's Earth Observation for Sustainable Development of Forests (EOSD) classification was used to analyze trends in NDVI by cover type for portions of the time series transect south of tree line (http://www4.saforah.org/eosdlcp/nts_prov.html). Land cover information from the two classification products was merged to create a harmonized classification for the study region with six vegetation classes, barren or exposed bedrock, and water (Table 1). Trends were further analyzed by latitude by comparing the mean NDVI trend between adjacent (north-south) scenes. Trends in NDVI and temperature were tested for correlation with latitude using Pearson's product-moment correlation coefficient.

Finally, trends in Landsat NDVI for each cover type were further evaluated by slope, aspect, and elevation. Topographic information was derived from the Shuttle Radar Topography Mission (SRTM) 3 Arc Second Filled Finished-B product (USGS 2006; www.landcover.org). The relationship between slope, elevation, and aspect with positive non-disturbed NDVI trend occurrence was explored for a random sample of positive and no-trend observations (equal to 10% of total observations of each) using a binomial generalized linear model (R version 2.11.0, R Core Development Team 2010).

3. Results

The Landsat study area covered 26 million ha in a transect across the forest-tundra biome boundary. Approximately 70% of the transect had a sufficient number of cloud-free Landsat observations to assess trends in peak-season NDVI. Of this "observable" portion, one-third (34%) of the area experienced a statistically significant trend in NDVI during 1986 – 2010 based on the T-test criterion (Fig. 3a). The remaining observable area either had small NDVI trends that were not significantly different from zero or exhibited significant year-to-year variability that precluded statistical confidence.

Almost all of the statistically significant NDVI trends were positive. Large-scale forest disturbance events prior to or during the study period, including forest fires and timber harvests, accounted for 3.2% of the area with significant NDVI trends. Excluding these disturbances, 98.95% of the remaining trend area had positive (greening) trends and only 1.05% of the trend area exhibited negative (browning) NDVI trends (Fig. 3a). The mean positive trend was an increase 0.007 NDVI yr^{-1} for a total increase of 0.17 NDVI over the entire 24-year time series (Fig. 3b). Positive NDVI trends were concentrated north of the treeline; nearly half (48%) of the observed area north of treeline had a statistically significant positive NDVI trend compared to only 25% of observable area south of treeline. Latitude and the frequency of statistically significant NDVI trends were positively correlated (Pearson's R = *0.819*, P = *0.0248*), although the magnitude of the NDVI trend was not correlated with latitude (Fig. 4, Table 2). Temperature trends, both annual and cumulative, were not significantly correlated with trends in NDVI abundance or magnitude (Table 2).

245 NDVI trends showed significant associations with specific land cover types (Fig.5, Table 3).
246 Low shrubs and graminoid tundra contributed preferentially to the observed greening trend. Out
247 of the area showing a positive NDVI trend, 38% occurred in regions classified as either
248 low/dwarf shrubs or graminoid tundra, even though these types only make up 22% of the study
249 area. Within the total area of tall shrubs, 30% of observations showed a positive trend. The rate
250 of NDVI increase for all cover types was broadly similar, varying from 0.0055 NDVI year $^{-1}$ for
251 sparsely vegetated areas to 0.0075 NDVI yr^{-1} for graminoid tundra. Although forests comprise
252 the majority of the southern portion of the transect, they contributed less than 10% to the overall
253 greening trend. Within forests, 15% of total observations showed a positive trend, with a mean
254 increase of 0.0064 NDVI yr^{-1}. In contrast, 50-60% of the low/dwarf shrub and graminoid tundra
255 areas showed significant NDVI increases.
256
257 Positive trends in peak summer NDVI correspond to an increase in LAI over time. Using
258 MODIS data for the study region, statistically significant changes in NDVI between 0.005 - 0.01
259 yr^{-1} corresponded to changes in LAI of ~0.02 (mode) to 0.03 (median) LAI yr^{-1} (Fig. 6). This
260 relationship between MODIS LAI and NDVI was invariant across the multiple cover types
261 occurring in the study region. We applied a value of 0.025 LAI yr^{-1} to those Landsat NDVI
262 trends not associated with disturbance, assuming that areas not exhibiting significant trends
263 experienced no change in LAI. The resulting estimate of the area-averaged LAI change across
264 the transect was 0.2 LAI over the 24-year record. However, for tundra cover types in the
265 northern portion of the transect, the estimated 24-year LAI increase was *ca*. 0.3. Tundra and
266 shrub-tundra LAI values generally fall in the range of 0.5 to 1.5 (Asner *et al.* 2003; Beringer *et*

al. 2005; Williams 2008), thus an LAI increase of 0.3 translates to roughly a ~20-60% increase in leaf area over two decades.

Geographically, the highest magnitude of NDVI change occurred proximal to and north of the regional treeline, which roughly coincides with the Rivière aux Feuilles (Fig. 3b). Greening trends were less abundant in the forested regions in the southern half of the transect, and trends decayed in frequency and magnitude along the northern edge bordering the Hudson Strait.

Topography was an important predictor of greening trends over the study domain (Table 4). While the landscape is generally flat, locations with higher slopes and elevations were negatively correlated with the frequency of detecting greening trends. North- and northeast- facing slopes were least likely to exhibit a positive trend, and western and southwestern facing slopes were the most likely. Stronger NDVI trends were detected along two major rivers, the Rivière aux Feuilles and the southern reaches of the Rivière Arnaud. Topographic associations between valley bottoms and vegetation growth likely reflect more favorable edaphic conditions along the channel banks, as well as more sheltered microclimates and available water.

Most cover types exhibited consistent linear changes in NDVI over the 24-year study period. The temporal distribution of the Landsat images did not support a regional, year-by-year analysis of greening trends. Instead, we divided observations into “early” (1985-1990), “mid” (1998-2001), and “late” (2008-2010) intervals to evaluate rates of NDVI change by cover type over time (Fig. 7). Most classes maintained similar rates of NDVI change during both early and late intervals. However, in wetland and tall shrub classes, NDVI increases were slower in the later period.

4. Discussion

Using time series of Landsat data, we found a strong mid-summer greening trend across the northern Quebec area. This trend corresponds to significant increases in peak growing season leaf area. Graminoid and shrub-tundra classes contributed nearly 60% of the greening trends identified in this study. These low-biomass vegetation types experienced a 20-60% relative increase in green leaf area over the 24-year study period—a rapid and significant increase relative to existing phytomass. Whether these LAI gains reflect the growth of individual plants, an increase in the density of individuals, or community-scale changes such as shifts from graminoid- to shrub-dominated tundra remains an important area for further study. Large and persistent changes in LAI identified in this study may also alter biophysical feedbacks, including seasonal changes in albedo (e.g., Randerson *et al.* 2006; Bonan 2008), snow cover, and turbulent fluxes (e.g., Lee *et al.* 2011).

Changes in shrub and graminoid tundra in this study are consistent with regional evidence of shrub expansion in tundra ecosystems (Ropars & Boudreau, 2012) and similar findings across North America (Chapin 1995, Sturm *et al.* 2001; Tape *et al.* 2006, Jagerbrand 2005; Van Wijk *et al.* 2004). A recent air photo analysis for a region west of our transect revealed increases in dwarf birch (*Betula glandulosa* Michx.) shrub cover up to 47% over a 51-year period (1957-2008), with larger changes on low-altitude sandy terraces than on exposed hilltops (Ropars & Boudreau, 2012). The Landsat data suggest that this shrub expansion is not isolated, but widespread across the tundra region of northern Quebec. Quebec and Alaska were the only regions in North America with strong warming trends in both winter and summer semesters

during 1970-2009, and both regions have consistent reports of increasing shrub cover during the satellite era. We did not identify strong correlations between the magnitude of recent temperature changes and increases in fractional cover, possibly due to consistent and strong (1.5°-2.5°) warming across the entire study region. Given favorable climatic conditions, landscape heterogeneity and species-level responses may be stronger predictors of vegetation change.

Biophysical mechanisms operating at the local scale may contribute to observed NDVI/LAI increases in tundra cover types. First, snowdrifts are more likely to form at lower elevations, trapping organic debris and leaf litter (Fahnestock *et al.* 2000). Snow protects newly-established shrubs from harsh winter conditions, and warmer soil temperatures under deep snow may increase microbial activity that mobilizes additional nutrients for shrub growth (Sturm *et al.* 2005). A positive feedback between shrub cover and snow is consistent with larger LAI increases at lower slopes and elevations in this study. In more sparsely vegetated cover types, dominated by lichen, mosses, and bryoids, another feedback cycle between the lichen-caribou-woody plant communities may be important. Caribou trampling destroys the lichen and exposes mineral soil, allowing for an increase in seedling establishment for dominant subarctic tree and shrub species such as black spruce (*Picea mariana*; Dufour-Tremblay & Boudreau 2011) and dwarf birch (*B. glandulosa;* Ropars & Boudreau, 2012). The activity of the Leaf River Caribou Herd in western subarctic Quebec peaked during the mid-1990s to mid-2000s (Dufour-Tremblay & Boudreau, 2011; Alexandre Truchon-Savard, pers. comm.), suggesting that browsing and soil disturbances from large herbivores may contribute to the patterns of shrub and graminoid tundra changes in this study. The availability of bare soil, whether from caribou disturbance or other

disturbances like frost boils or cryoturbation, combined with milder conditions more favorable for seed production and seedling establishment, may allow for the encroachment of woody species and other vascular vegetation into sparsely vegetated areas.

This study found less conclusive evidence for vegetation changes within forest areas. While most observations of NDVI trend within the forested parts of the transect were positive, a much smaller area showed a statistically significant trend compared to graminoid- and shrub-dominated regions. In contrast to the shrub expansion studies, evidence for northern advance of treeline into tundra has been mixed (Harsch *et al.* 2009). At the treeline, a positive temperature trend may not necessarily correlate with the northward expansion of trees, given the influence of water availability, soil properties, competition, or pests on the spatial arrangement of trees (Meunier *et al.* 2007). Furthermore, the responsiveness of non-tree species in forest communities, such as shrubs, to a positive temperature trend may be suppressed by tree cover (Boudreau & Villenueve-Simard 2012). Although within-stand changes in forest leaf area were less common, it is possible that expansion of tree species into tundra communities dominated by tall shrubs or other functional groups contributed some of the observed changes in other vegetation classes reported in the study. Additional field studies in areas of recent change are needed to identify the contributions from the growth of existing individuals (Gamache & Payette 2004; Beck *et al.* 2011) and establishment of new individuals (e.g., Danby & Hik 2007) to recent increases in vegetation cover.

Observed NDVI trends in forest may reflect recovery from historic disturbances, despite efforts to mask out large-scale disturbances from fires and forestry operations visible during the Landsat

era. In eastern Canada, severe fires sharply reduce LAI, and vegetation regrowth occurs over century timescales, during which post-fire succession is likely to overshadow climate-driven trends in vegetation (Girard *et al.* 2008). Two other factors may contribute to the lack of observed forest greening within a time series of Landsat data. First, the establishment and growth of trees is an inherently slower process compared to growth of existing individuals (e.g., Danby & Hik 2007), and the 24-year Landsat record may not be long enough to identify changes within forest stands. Second, forested areas tend to have higher initial NDVI values. Since NDVI saturates at modest LAI values (~3.0), small LAI increases within existing forest stands may not be obvious from the remote sensing data.

DGVMs suggest poleward migration of biomes as a long-term response to climate warming (Lucht *et al.* 2006). The observed association between shrub cover types and increased NDVI is generally consistent with the concept that woody plants can take advantage of warmer conditions and grow more vigorously. In areas of mixed graminoid and shrub cover types, the competitive advantage of shrubs should lead to a long-term shift in composition, and ultimately a poleward shift in the biome boundary. However, the satellite data do not yet provide unambiguous evidence for geographic biome shifts as opposed to simply increasing LAI within existing biome distributions. As noted by others, the ability of vegetation communities to expand their range depends not just on increased productivity, but on overcoming a host of ecological constraints (Rozensweig *et al.* 2008). Particularly in the boreal environment of Canada, small lakes and rocky outcrops present innumerable fine-scale barriers to propagation and expansion. The poor reproductive capacity of frontier tree species such as *Picea mariana* may also somewhat explain observed lags between warming and vegetation growth, both above and below the subarctic

383 treeline (Gamache & Payette 2004), although an increase in seed viability was noticed near the
384 treeline in recent years (Dufour-Tremblay & Boudreau, 2011). These fine-scale barriers to forest
385 expansion constitute macro-scale “resistance” to biome shifts that are not considered in the
386 current generation of DGVMs.
387
388 Our results complement previous studies of high-latitude vegetation change using moderate or
389 coarse-resolution satellite data (e.g., Pouliot *et al.* 2009). We used Landsat time series to
390 subdivide the overall greening trend into increases in LAI for specific cover types. The Landsat-
391 based approach in this study could be expanded to evaluate climate-driven shifts in vegetation in
392 other regions, within the limits of the existing Landsat data archive (Goward *et al.* 2006). High-
393 resolution time series over the 35+ year Landsat record provide invaluable observational data to
394 refine and benchmark ecological models. However, there are several important limitations of
395 this work that could be addressed in future studies. First, given the uncertainties in the MODIS
396 LAI product in high-latitude areas, the uncertainties in the derived MODIS NDVI-LAI
397 relationship, and the difficulties of scaling field-observed LAI to satellite resolution, area-
398 averaged LAI increases in this study should be interpreted cautiously. Second, we evaluated
399 trends in Landsat NDVI by cover type using vegetation classification data from a snapshot in
400 time (circa 2000). Classification information from 2000 may already incorporate growth of
401 woody vegetation during 1986-2000, such that areas classified as shrublands in 2000 had lower
402 amounts of woody cover at the beginning of the study period. Third, multispectral remote
403 sensing has limited sensitivity to subtle changes in composition and structure, especially in
404 closed-canopy forest conditions. The addition of hyperspectral imagery (to map compositional
405 gradients) and LiDAR(to map structure) would provide a more comprehensive benchmark of

406 current conditions for future studies of climate-driven vegetation changes. Finally, we identified
407 linear changes in NDVI over the Landsat study domain. Non-linear greening or browning
408 responses to recent climate warming may therefore be underestimated in this study.
409
410 Using time series of Landsat observations, we mapped widespread vegetation greening in
411 northern Quebec over the last 24 years. The observed NDVI increases were concentrated in
412 graminoid and shrub-tundra areas, leading to an area-averaged LAI increase of ~0.2 across the
413 entire transect, or ~0.3 for the northern tundra-dominated portion. The latter figure represents a
414 20-60% relative increase compared to typical shrub-tundra LAI values. These findings expand
415 the spatial extent of previous field and air photo studies used to characterize changes in shrub
416 cover. Our results also provide a fine-scale evaluation of the contribution of different cover
417 types to trends detected from coarse-resolution satellite data. The coincidence of the shrub
418 greening trend with an area of rapid winter and summer warming supports the hypothesis that
419 warmer temperatures favor the growth of woody plants at high latitudes (Sturm *et al.* 2001;
420 2005; Tape *et al.* 2006). In contrast, positive NDVI trends within forested areas were less
421 common, suggesting that the forest response to recent warming may be occurring more slowly,
422 or that Landsat data alone may be insufficient to identify growth responses in these ecosystems
423 and additional data (e.g., LiDAR) may be needed to characterize temperature-induced vegetation
424 changes within boreal forest communities.
425
426

6. Acknowledgements

This work was supported by the NASA Terrestrial Ecology Program. We thank M.A. Wulder for guidance on land cover information for eastern Canada, and we appreciate comments and suggestions on a previous version of this manuscript from H. Margolis and an anonymous reviewer.

7. References

Asner GP, Schurlock J, and Hicke JA (2003) Global synthesis of leaf area index observations: implications for ecological and remote sensing studies. *Global Ecology & Biogeography*, **12**, 191-205.

Beck SA, Horning S, Goetz SJ, Loranty MM, Tape KD (2001) Shrub Cover on the North Slope of Alaska: a circa 2000 Baseline Map. *Arctic, Antarctic, and Alpine Research* **43**, 355-363.

Beringer J, Chapin FS, Thompson CC, McGuire AD (2005) Surface energy exchanges along a tundra-forest transition and feedbacks to climate. *Agricultural and Forest Meteorology*, **131**, 143-161.

Bonan GB (2008) Forests and Climate Change: Forcings, Feedbacks, and the Climate Benefits of Forests. *Science*, **320**, 1444-1449.

Boudreau S & Villeneuve-Simard MP (2012) Dendrochronological evidence of shrub growth suppression by trees in a subarctic lichen woodland. *Botany* **90**, 151-156.

Bunn AG & Goetz SJ (2006) Trends in satellite-observed circumpolar photosynthetic activity from 1982 to 2003: the influence of seasonality, cover type, and vegetation density. *Earth Interactions*, **10**, 1–19.

Chapin FS III, Shaver GR, Giblin AE, Nadelhoffer KJ, and Laundre JA (1995) Responses of arctic tundra to experimental and observed changes in climate. *Ecology*, **76**, 694–711.

Danby RK & Hik DS (2007) Variability, contingency and rapid change in recent subarctic alpine tree line dynamics. *Journal of Ecology*, **95**, 352-363.

Doufour-Tremblay G & Boudreau SB (2011) Black spruce regeneration at the treeline ecotone: synergistic impacts of climate change and caribou activity. *Canadian Journal of Forest,* **41**, 460-468.

Emanuel WR, Shugart HH, Stevenson MP (1985) Climate change and the broad scale distribution of terrestrial ecosystem complexes. *Climatic Chang,e* **7**: 29-43.

Gallo K, Ji L, Reed B, Eidenshink J, Dwyer J (2005). *Remote Sensing of the Environment,* **99**, 221-231.

Gamache I & Payette S (2004) Height growth response of tree line black spruce to recent climate warming across the forest-tundra of eastern Canada. *Journal of Ecology*. **92,** 835-845.

Girard F, Payette S, Gagnon R (2008) Rapid expansion of lichen woodlands within the closed-crown boreal forest zone over the last 50 years caused by stand disturbances in eastern Canada. *Journal of Biogeography*. **35,** 529-537.

Goetz SJ, Bunn AG, Fiske GJ, Houghton RA (2005) Satellite-observed photosynthetic trends across boreal North America associated with climate and fire disturbance. *Proceedings of the National Academies of Science,* **102**, 13521-5.

Goward S, Arvidson T, Williams D, Faundeen J, Irons J, Franks S (2006) Historical record of Landsat global coverage: Mission operations, NSLRSDA, and international cooperator stations. *Photogrammetric Engineering & Remote Sensing,* **72**, 1155-1169.

Harsch MA, Hulme PE, McGlone MS, Duncan RP (2009) Are treelines advancing? A global meta-analysis of treeline response to climate warming. *Ecology Letters,* **12**, 1040–1049.

Harsch MA & Bader MY (2011) Treeline form – a potential key to understanding treeline dynamics. *Global Ecology and Biogeography,* **20:**582-596.

Huete A, Didan K, Miura T, Rodriguez EP, Gao X, Ferreira LG (2002) Overview of the radiometric and biophysical performance of the MODIS vegetation indices. 195-213.

IPCC (2007) *Climate change 2007:Impacts, adaptation and vulnerability. Contribution of Working Group II to the Fourth Assessment Report of the Intergovernmental Panel on Climate Change* Parry ML, Canziani OF, Palutikof JP, van der Linden PJ, Hanson CE, eds. Cambridge University Press: 211-272.

Jagerbrand AK, Lindblad KEM, Bjork RG, Alatao JM, Molau U (2006) Bryophyte and lichen diversity under simulated environmental change compared with observed variation in unmanipulated alpine tundra. Biodiversity and Conservation, **15,** 4453-4475.

Knyazikhin Y, Glassy J, Privette JL, *et al.* MODIS Leaf Area Index (LAI) and Fraction of Photosynthetically Active Radiation Absorbed by Vegetation (FPAR) Product (MOD15) Algorithm, Theoretical Basis Document,126 pp., NASA Goddard Space Flight Center, Greenbelt, Md., 1999.

Kullman L (2001) 20th Century Climate Warming and Tree-Limit Rise in the Southern Scandes of Sweden. *Ambio,* **30**, 72-80.

Lee X, Goulden ML, Hollinger DY, *et al.* (2011) Observed increase in local cooling effect of deforestation at higher latitudes. *Nature,* **479**, 384-387.

Lucht W, Schaphoff S, Erbrecht T, Heyder U, Cramer W (2006). Terrestrial vegetation redistribution and carbon balance under climate change. *Carbon Balance and Management,* **1,** 1-6.

Markham BL & Helder D (in press) Forty-year calibrated record of earth-reflected radiance from Landsat: a review, *Remote Sensing of the Environment.*

Masek JG (2001) Stability of boreal forest stands during recent climate change: evidence from Landsat satellite imagery. *Journal of Biogeography,* **28**, 967-976.

Masek JG, Vermote EF, Saleous N, *et al.* (2006) A Landsat surface reflectance data set for North America, 1990-2000. *Geoscience and Remote Sensing Letters,* **3**, 68-72.

Meunier C, Sirois L, Bégin Y (2007) Climate and *Picea mariana* seed maturation relationships: a multi-scale perspective. *Ecological Monographs,* **77**, 361-376.

Mitchell TD & Jones PD (2005) An improved method of constructing a database of monthly climate observations and associated high-resolution grids. *International Journal of Climatology,* **25**, 693-712.

Myneni RB, Keeling CD, Tucker CJ, Asrar G (1997) Increased plant growth in the northern high latitudes from 1981to 1991. *Nature,* **386**, 698-702.

Pastor J & Post WM (1988) Response of northern forests to CO_2-induced climate change. *Nature,* **334**, 55-58.

Parmesan C & Yohe G (2003) A globally coherent fingerprint of climate change impacts across natural systems. *Nature,* **421**, 37-42.

Pouliot D, Latifovic R, Olthof I (2009) Trends in vegetation NDVI from 1 km AVHRR data over Canada for the period 1985-2006. *International Journal of Remote Sensing,* **30,** 149-168.

Prentice KC & Fung IY (1990) The sensitivity of terrestrial carbon storage to climate change. *Nature,* **346**, 48–50.

Randerson JT, Liu H, Flanner MG, *et al.* (2006) The impact of boreal forest fire on climate warming. *Science*, **314**, 1130-1132.

Ropars P, & Boudreau S (2012) Shrub expansion at the forest-tundra ecotone: spatial heterogeneity linked to local topography. *Environmental Research Letters* **7** (015501).

Rosenzweig C, Karoly D, Vicarelli M, *et al*. (2008) Attributing physical and biological impacts to anthropogenic climate change. *Nature*, **453**, 353-357.

Running SW, Nemani RR, Heinsch FA, Zhao M, Reeves M, Hashimoto H (2004). A continuous satellite-derived measure of global terrestrial primary production. *BioScience,* **54,** 547:560.

Sturm M, Racine C, Tape K (2001) Climate change – increasing shrub abundance in the Arctic. *Nature*, **411**, 546–547.

Sturm M, Schimel J, Michaelson G, Welke JM (2005) Winter biological processes could help convert Arctic tundra to shrubland. *Bioscience,* **55**,17-26.

Tape K, Sturm M, Racine C (2006) The evidence for shrub expansion in Northern Alaska and the Pan-Arctic. *Global Change Biology,* **12**, 686–702.

Tremblay B (2010) Augmentation récente du couvert ligneux érigé dans les environs de Kangiqsualujjuaq (Nunavik, Québec). MSc thesis, Université du Québec à Trois-Rivières, Trois-Rivières, Québec, Canada.

Tucker CJ (1979) Red and Photographic Infrared Linear Combinations for Monitoring Vegetation, *Remote Sensing of Environment*, **8**,127-150.

Turner DP, Cohen WB, Kennedy RE, Fassnacht KS, & Briggs JM (1999) Relationships between leaf area index and Landsat TM spectral vegetation indices across three temperate zone sites. *Remote Sensing of Environment*, **70**, 52–68.

University of East Anglia Climatic Research Unit (CRU) [Phil Jones, Ian Harris]. CRU Time Series (TS) high resolution gridded datasets, [Internet]. NCAS British Atmospheric Data Centre, 2008. http://badc.nerc.ac.uk/view/badc.nerc.ac.uk__ATOM__dataent_1256223773328276

Van Wijk MT, Clemmensen KE, Shaver GR, *et al*. (2004) Long-term ecosystem level experiments at Toolik Lake, Alaska, and at Abisko, Northern Sweden: generalizations and differences in ecosystem and plant type responses to global change. *Global Change Biology*, **10**, 105 -123 .

Wang D, Morton D, Masek J, *et al*. (2012) Impact of sensor degradation on the MODIS NDVI time series. *Remote Sensing of Environment*.**119**, 55-61.

Wang X, Piao S, Ciais P, Li J, Friedlingstein P, Koven C, Chen A (2011) Spring temperature change and its implication in the change of vegetation growth in North America from 1982 to 2006. *Proceedings of the National Academies of Science*, **108**, 1240-1245.

White A, Cannell MGR, Friend AD (2000) The high-latitude terrestrial carbon sink: a model analysis. *Global Change Biology*, **6**, 227-245.

Williams M, Bell R, Spadavecchia L, Street LE, van Wijk MT (2008) Upscaling leaf area index in an Arctic landscape through multi-scale observations. *Global Change Biology*, **14**, 1517-1530.

Zhang X, Friedl MA, Schaaf CB, Strahler AH, Hodges JCF, Gao F, Reed B, Huete A (2003) Monitoring vegetation phenology using MODIS. *Remote Sensing of Environment*, **84,** 471-475.

Zhao M and Running SW (2010) Drought-Induced Reduction in Global Terrestrial Net Primary Production from 2000 Through 2009. *Science*, **329**, 940 – 943.

Table 1. Harmonization scheme for a simplified vegetation classification of the study area, based upon the Canadian Centre for Remote Sensing (CCRS) Northern Land Cover of Canada and the Canadian Forest Service Earth Observation for Sustainable Development of Forests (ESOD) datasets.

CCRS classification	EOSD classification	Harmonized Classification
Tussock graminoid tundra	Herbaceous (grasses, crops, forbs, graminoids; 20% ground cover)	**Graminoid**
Wet sedge		
Moist to dry non-tussock graminoid/ dwarf shrub tundra		**Low & dwarf shrub**
Prostrate dwarf shrub		
Low shrub (< 40cm; >25% cover)		
Tall shrub (>40cm; >25% cover)	Shrub- tall (>2m; 20% ground cover)	**Tall shrub**
	Shrub- low (<2m; 20% ground cover)	
	Coniferous: Dense, Open, and Sparse[1]	**Forest**
	Broadleaf: Dense, Open, and Sparse[1]	
	Mixed Wood: Dense, Open, and Sparse[1]	
Sparsely vegetated bedrock	Bryoids (bryophytes and lichen; 20% ground cover or 1/3 of vegetation)	**Sparse vegetation**
Sparsely vegetated till-colluvium		
Bare soil with cryptogam crust-frost boils		
Wetlands	Wetland- Coniferous	**Wetlands**
	Wetland- Broadleaf	
	Wetland- Mixed Wood	
	Wetland- Shrub- Tall	
	Wetland- Shrub- Low	
Barren	Rock/rubble	**Barren & exposed surfaces**
	Exposed land (<5% vegetation)	
Water	Water	**Water**
Ice/snow	Cloud	**No data**
Shadow	Shadow	
No data	Snow/ice	
	No data	

[1] Coniferous, broadleaf, and mixed wood classes were further subdivided in the EOSD classification as dense (>60% crown closure), open (26-60% crown closure), and sparse (10-25% crown closure).

628

Table 2. Correlation coefficients for the relationships among latitude, summer and winter temperature (T) changes (1970-2009), and Landsat NDVI trends (1986-2010), summarized at 0.5° resolution.

Variables	Latitude	Winter T Change	Summer T Change
Latitude	-		
Winter T Change	0.39	-	-
Summer T Change	0.47	-	-
Fraction + NDVI Trend	0.82*	0.19	0.28
Fraction - NDVI Trend	-0.71	-0.56	-0.64
Fraction no NDVI Trend	-0.81*	-0.17	-0.26
Positive NDVI Trend	-0.62	-0.04	-0.19
Negative NDVI Trend	-0.34	-0.23	-0.38

* p <0.05; ** p <0.01; *** p <0.001

629

630

Table 3. Positive Landsat NDVI trends by land cover class for the Quebec study region.

Class	Fraction of study area	Fraction of positive NDVI trend area	Fraction of class with positive NDVI trend	Mean annual positive NDVI trend (±1S.D.)
Barren and exposed surfaces	8.0	8.1	35.0	$6.0 \times 10^{-2} \pm 2.2 \times 10^{-2}$
Sparse vegetation	16.5	15.7	32.7	$5.5 \times 10^{-2} \pm 2.8 \times 10^{-2}$
Tall shrubs	25.6	23.1	31.0	$7.5 \times 10^{-2} \pm 3.5 \times 10^{-2}$
Wetlands	2.5	2.1	28.7	$5.9 \times 10^{-2} \pm 3.9 \times 10^{-2}$
Forest	20.9	9.7	16.0	$6.4 \times 10^{-2} \pm 3.8 \times 10^{-2}$
Low and dwarf shrubs	14.1	23.1	56.5	$6.3 \times 10^{-2} \pm 2.3 \times 10^{-2}$
Graminoid	8.3	14.6	60.8	$7.5 \times 10^{-2} \pm 2.7 \times 10^{-2}$
Water	4.2	3.5	28.2	$5.6 \times 10^{-2} \pm 2.4 \times 10^{-2}$

631

Table 4. Topographic coefficients derived from generalized linear model (GLM) fit of greening trends. Based upon Landsat data from 1985-2010 for northern Quebec.

Binomial GLM: Positive non-disturbed trend/no trend.	
	Estimate[c]
Intercept	1.282
Slope[a]	-0.03651
Elevation[a]	-0.006545
Aspect[b]:	
Flat	-0.5449
N	-0.08753
NE	-0.1102
E	-0.1271
SE	-0.07817
S	-0.04362
SW	0.05415
W	0.08525
NW	NA
[a] *continuous;* [b]*ordinal*	
[c]*p-values for all variables < 2e-16*	

Fig. 1. Changes in mean winter (left) and summer (right) temperatures between 1970 and 2009 across Boreal North America based on the CRU TS3.1 dataset. The locations of the Landsat transect (white) and boreal forest biome (green) are also shown.

Figure 2. The temporal distribution of the Landsat data (1985-2010) used in this study. Each panel represents a frame (path-row location), and the images used are shown by year (x-axis) and day of year (y-axis). Images were selected within a window of peak greenness (day of year 185-215) whenever high quality, minimal cloud-covered images were available. Closed circles indicate Landsat-5 TM data; open circles indicate Landsat-7 ETM+ data.

Figure 3. a. Locations of positive, negative, and no NDVI trend across the study region, based upon Landsat data from 1985-2010 for northern Quebec. White regions signify that data were not in sufficient quantity to determine a statistical trend. Red regions denote areas of known disturbances; b. The magnitude of trend across the study region.

Figure 4. The mean annual NDVI trend by latitude (top). Trends in winter and summer temperatures (1970-2009) and fraction of NDVI change by latitude (bottom).

Figure 5. (left) The fraction of observable (non cloud) study area experiencing positive, negative, or no trend in Landsat NDVI (1986-2010); (right) distribution of land cover types among the area experiencing positive (greening) trend.

Figure 6. (a) Relationship between MODIS and Landsat NDVI (aggregated to 500m resolution) for pixels showing a statistically significant, positive NDVI trends; (b) Relationship between MODIS NDVI and LAI trends for the northern US and Canada. For the range of NDVI changes considered in this study (0.005-0.01 NDVI/yr), the corresponding modal and median values of LAI change are 0.02 and 0.03 LAI/yr, respectively.

Figure 7. Mean NDVI values per class for 1986, 2000, and 2010 reference periods. Data for each Landsat frame in the time series transect were selected within ±2 years of these reference years.

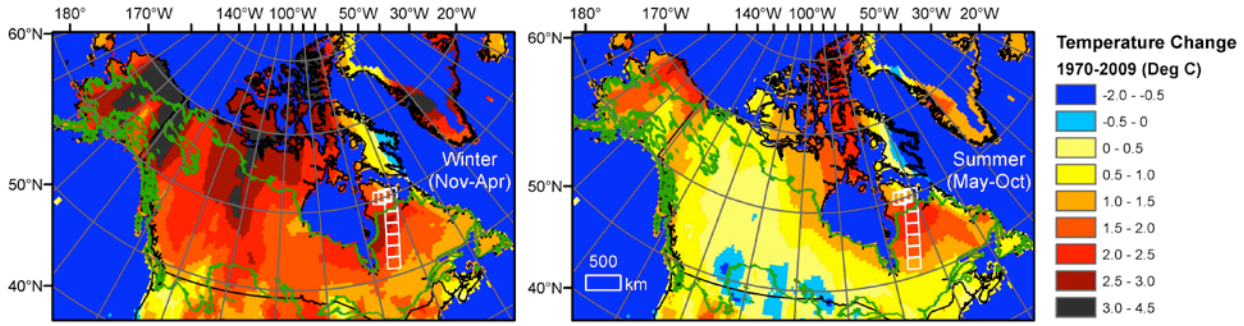

685
686 Fig. 1
687

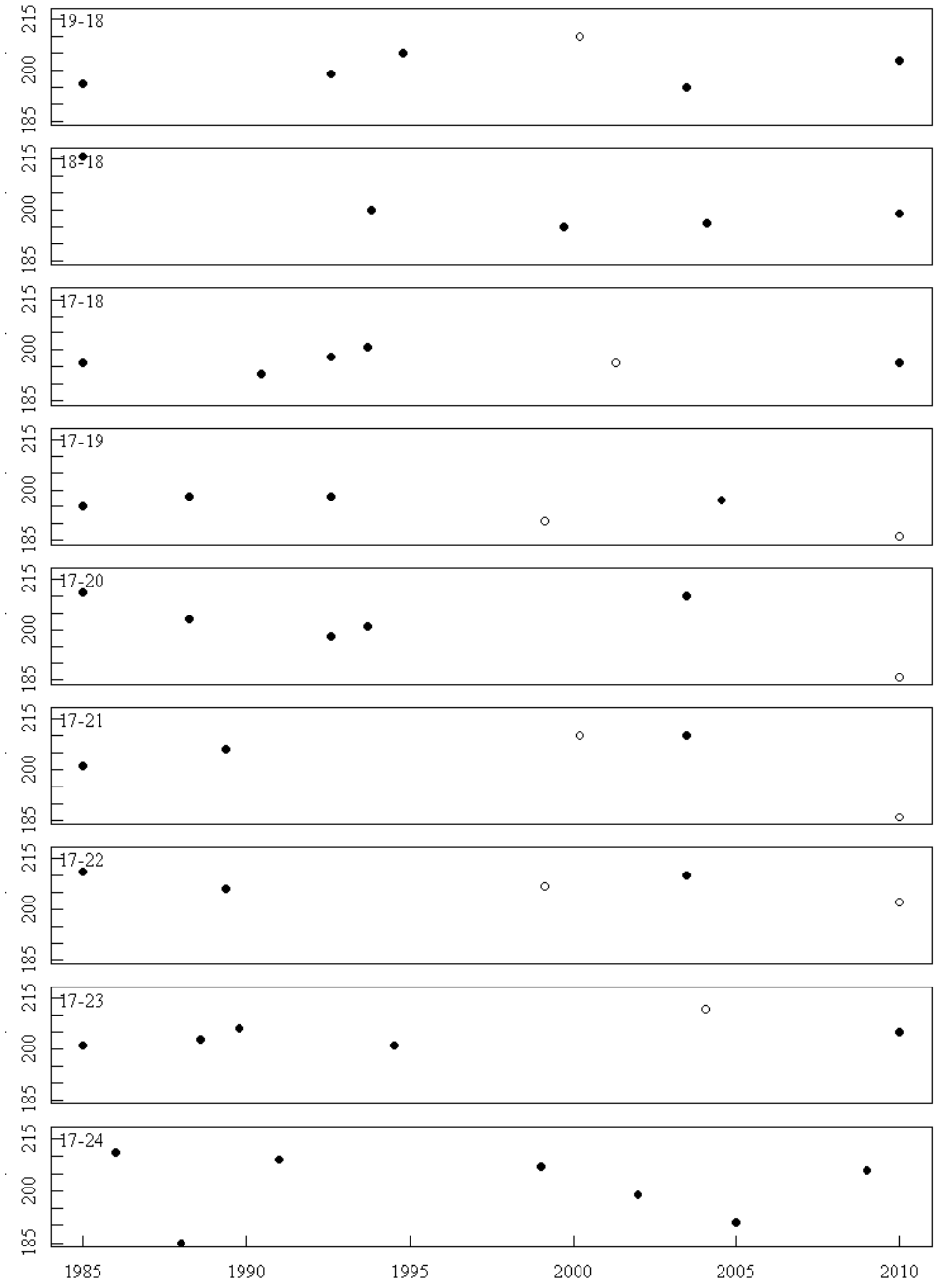
19-18
18-18
17-18
17-19
17-20
17-21
17-22
17-23
17-24
185
200
215
1985
1990
1995
2000
2005
2010

Fig. 2

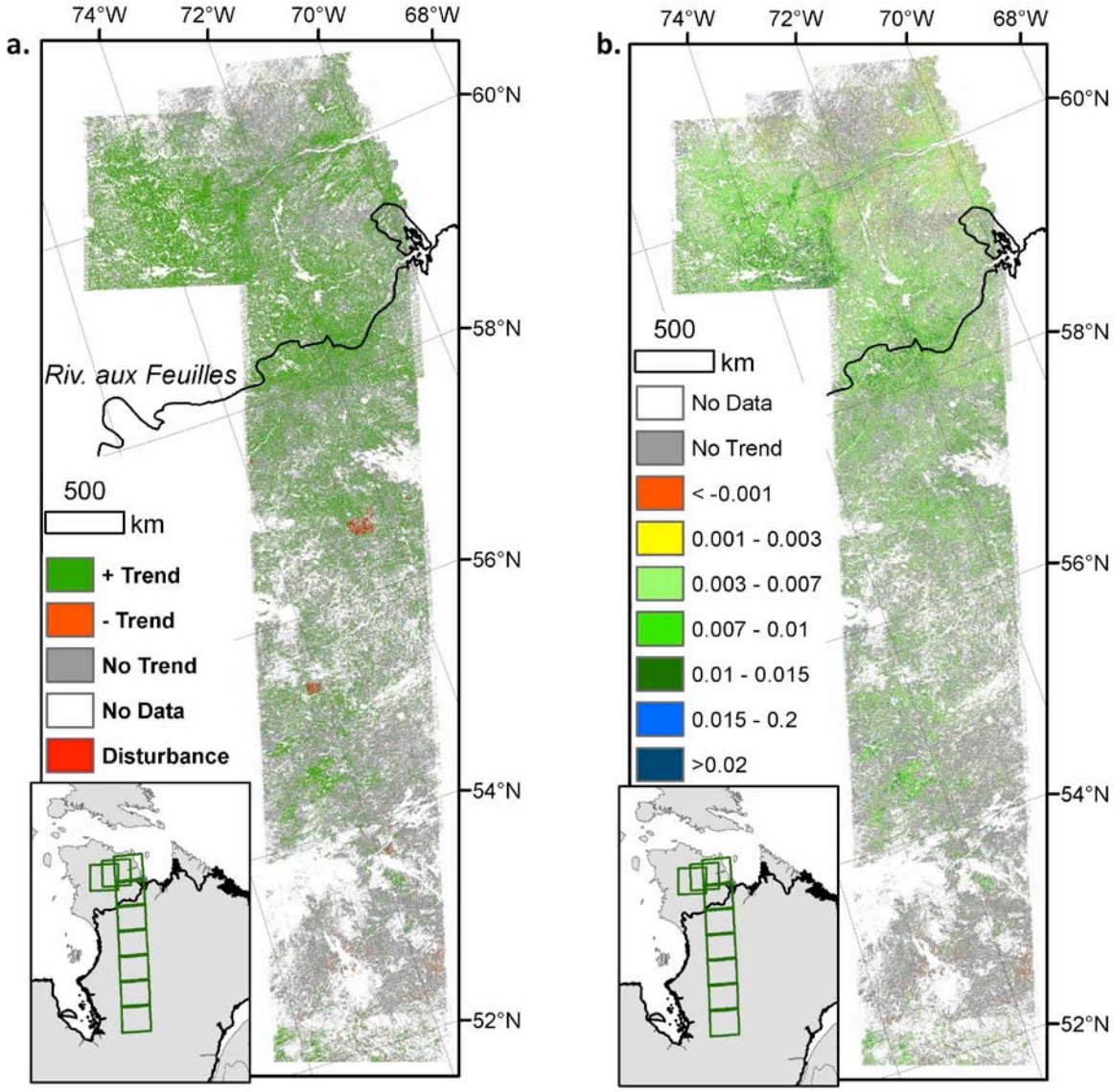

691
692 Fig. 3
693

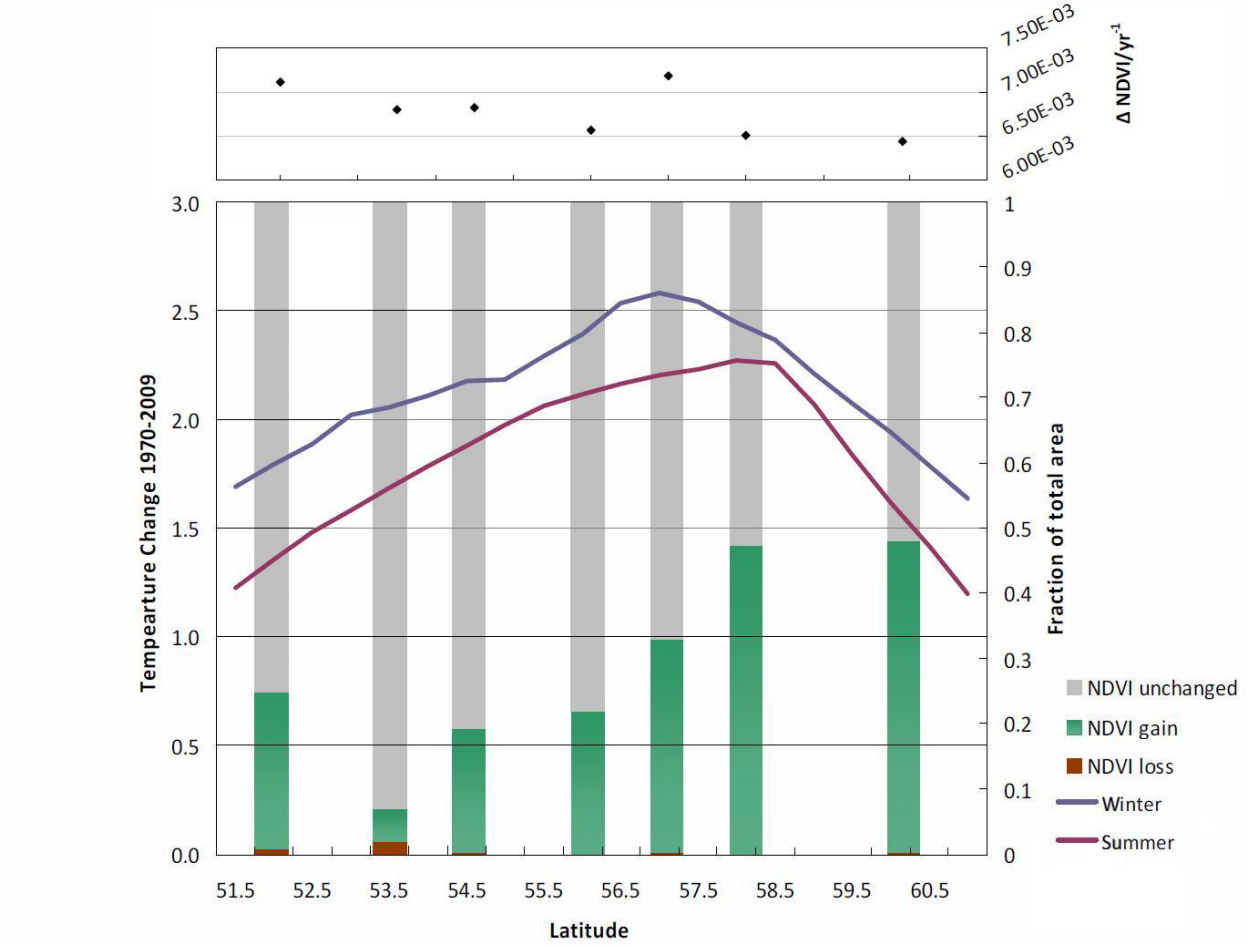

694
695 Fig 4.
696

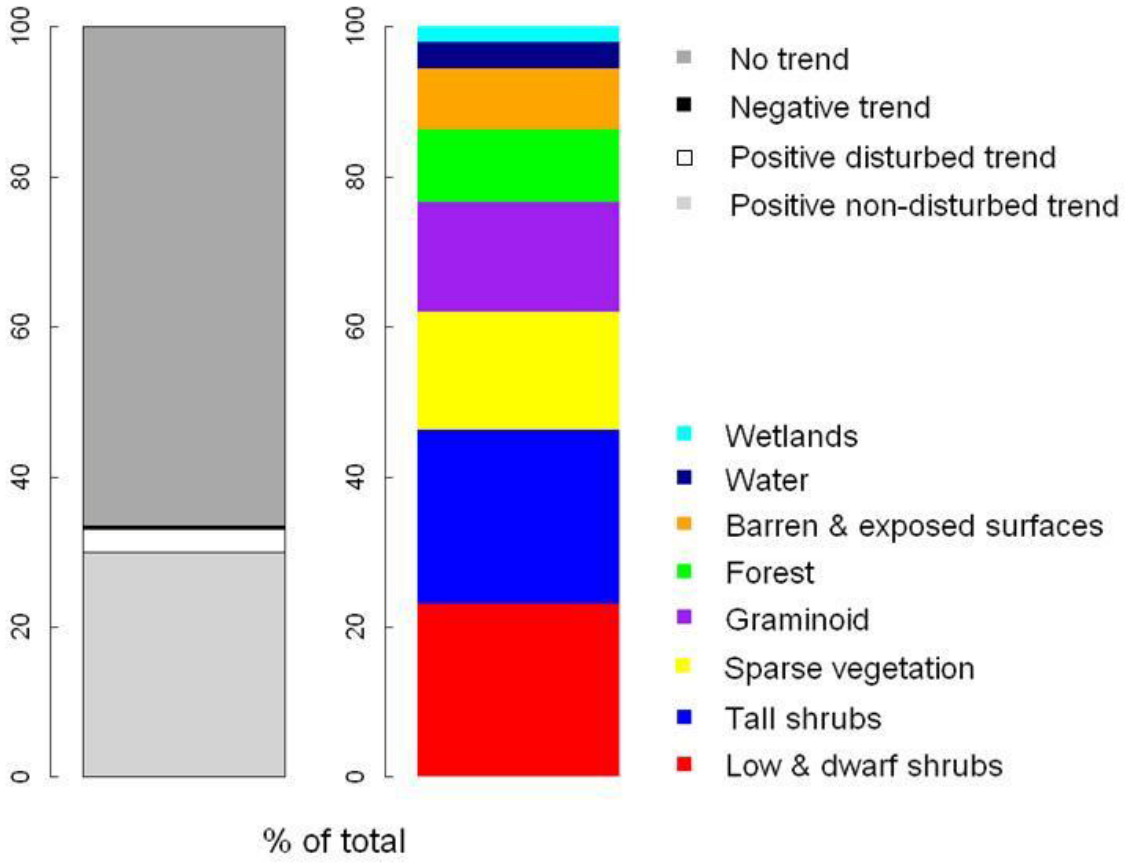
100
80
60
40
20
0
% of total
No trend
Negative trend
Positive disturbed trend
Positive non-disturbed trend
Wetlands
Water
Barren & exposed surfaces
Forest
Graminoid
Sparse vegetation
Tall shrubs
Low & dwarf shrubs

Fig. 5

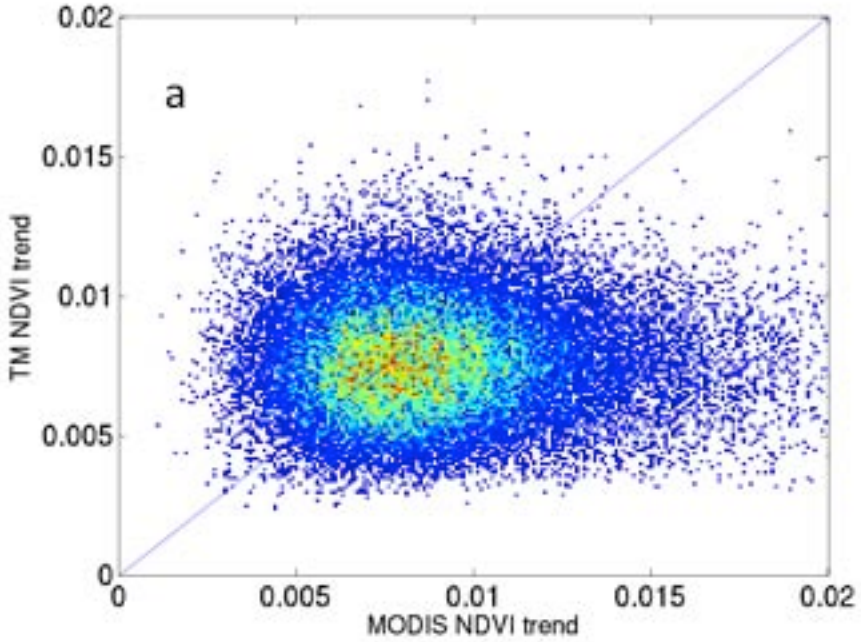

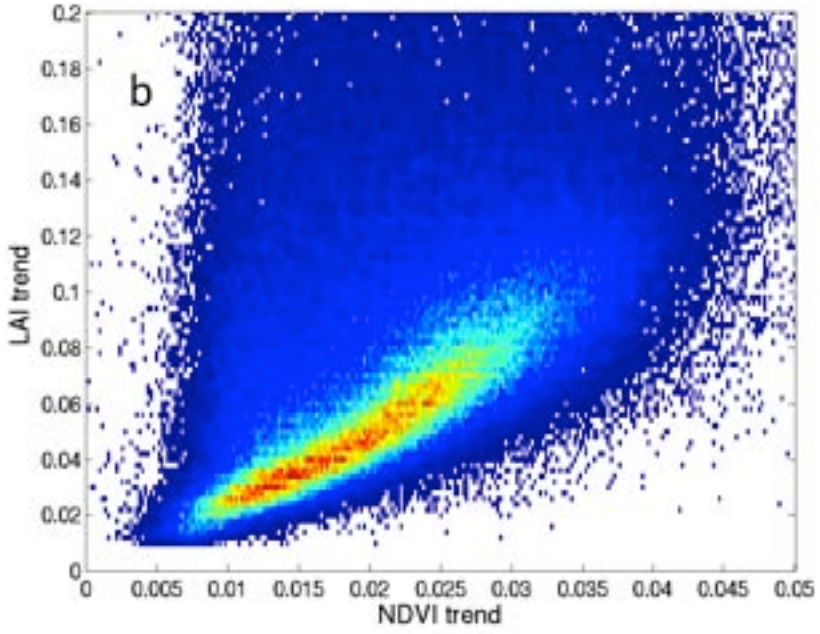

700
701 Fig. 6
702

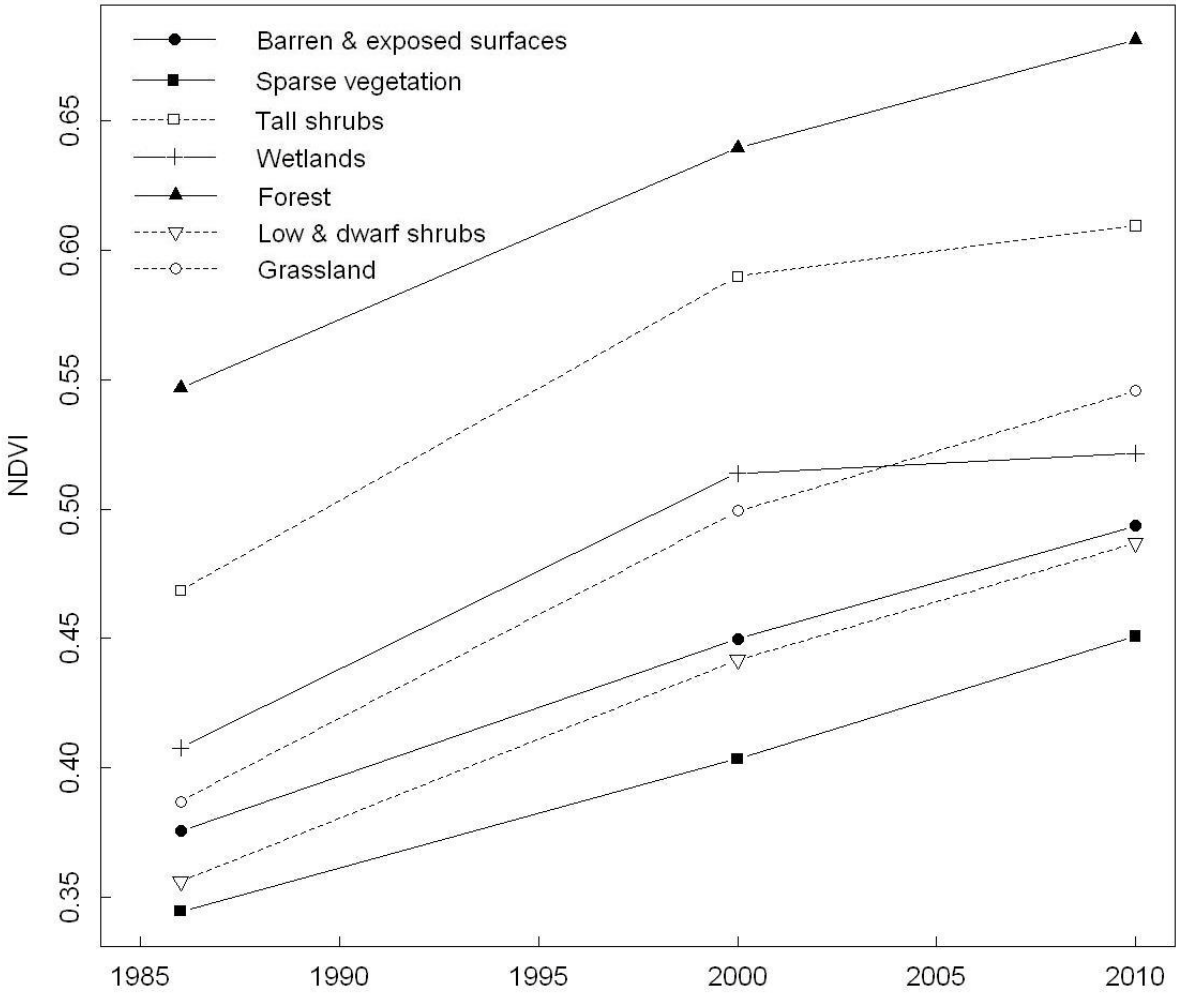
Barren & exposed surfaces
Sparse vegetation
Tall shrubs
Wetlands
Forest
Low & dwarf shrubs
Grassland
NDVI
0.35
0.40
0.45
0.50
0.55
0.60
0.65
1985
1990
1995
2000
2005
2010

703
704 Fig. 7